Saudi Journal of Biological Sciences 27 (2020) 1073–1079

Contents lists available at ScienceDirect

Saudi Journal of Biological Sciences

journal homepage: www.sciencedirect.com

Original article

Application of CT images in the diagnosis of lung cancer based on finite mixed model

Yuekao Li [a], Guangda Wang [a], Meng Li [a], Jinpeng Li [a], Liang Shi [a], Jian Li [b,*]

[a] Department of CT, The Fourth Hospital of Hebei Medical University, Shijiazhuang City, Hebei 050011, China
[b] Department of Radiology, Jining No. 1 People's Hospital, Jining City, Shandong Province 272000, China

ARTICLE INFO

Article history:
Received 11 October 2019
Revised 26 February 2020
Accepted 27 February 2020
Available online 4 March 2020

Keywords:
FMM
CT
Lung cancer
Segmentation of pulmonary nodules
Adaptive particle swarm optimization

ABSTRACT

Objective: Investigating the application of CT images when diagnosing lung cancer based on finite mixture model is the objective. Method: 120 clean healthy rats were taken as the research objects to establish lung cancer rat model and carry out lung CT image examination. After the successful CT image data preprocessing, the image is segmented by different methods, which include lung nodule segmentation on the basis of Adaptive Particle Swarm Optimization – Gaussian mixture model (APSO-GMM), lung nodule segmentation on the basis of Adaptive Particle Swarm Optimization – gamma mixture model (APSO-GaMM), lung nodule segmentation based on statistical information and self-selected mixed distribution model, and lung nodule segmentation based on neighborhood information and self-selected mixed distribution model. The segmentation effect is evaluated. Results: Compared with the results of lung nodule segmentation based on statistical information and self-selected mixed distribution model, the Dice coefficient of lung nodule segmentation based on neighborhood information and self-selected mixed distribution model is higher, the relative final measurement accuracy is smaller, the segmentation is more accurate, but the running time is longer. Compared with APSO-GMM and APSO-GaMM, the dice value of self-selected mixed distribution model segmentation method is larger, and the final measurement accuracy is smaller. Conclusion: Among the five methods, the dice value of the self-selected mixed distribution model based on neighborhood information is the largest, and the relative accuracy of the final measurement is the smallest, indicating that the segmentation effect of the self-selected mixed distribution model based on neighborhood information is the best.

1. Introduction

If the growth of lung tissue cells is uncontrolled, it will lead to a malignant lung tumor, like lung cancer (Yang et al., 2017). As one of the malignant tumors that pose the greatest threat to human health and life, its morbidity and mortality increase the fastest. If it is not treated, tumor cells will transfer to adjacent tissues as well as other parts of the body (Hui et al., 2017). According to histopathology, lung cancer includes small cell lung cancer (SCLC) as well as non-small cell lung cancer (NSCLC) (Timmeren et al., 2017). High risk factors for lung cancer include smoking, ionizing radiation, previous chronic pulmonary infection, air pollution, occupational and environmental exposure, and genetics, etc. (Lin et al., 2017). The clinical manifestations of the patients are relatively complex. According to the severity of the disease, cough, bloody sputum or hemoptysis, chest pain, fever, wasting and cachexia, or other extralopulmonary symptoms may occur (Li et al., 2017). Chest X-ray as well as CT scan can be used for the detection of lung cancer, and bronchoscopy or CT-guided biopsy can confirm it (Zhou et al., 2017). In the judgment of lung cancer, the size change of pulmonary nodules is an important basis (Vial et al., 2018).

CT images refers to the use of precise X-ray beam, γ rays, ultrasound and other extremely sensitive detectors around a specific part of the body to conduct cross section scanning one after another (Ostrowski et al., 2018). Due to its advantages of fast scanning time and clear image, it is widely used in the diagnosis of various diseases (Toyokawa et al., 2017). There is little difference in

* Corresponding author at: Department of Radiology, Jining No. 1 People's Hospital, Jiankang Road No 6, Shizhong District, Jining City, Shandong Province, China.
E-mail address: lijianjining@yeah.net (J. Li).
Peer review under responsibility of King Saud University.

Production and hosting by Elsevier

https://doi.org/10.1016/j.sjbs.2020.02.022
1319-562X/

the density of human soft tissue, while CT scan generates contrast images with its high-density resolution (Jacobson and Jaklitsch, 2018). Therefore, organs that are composed of soft tissue like brain, lung, liver as well as pelvic organs, etc. can be well displayed by CT. In addition, CT can show the lesion image on a good anatomical image background (Vial et al., 2018).

FMM is an effective mathematical method to simulate complex density with simple density, and it is a statistical modeling tool. Its core problems include selecting the distribution function of mixed components, accurately estimating the number of components of the mixed model, and estimating the parameters of the mixed model (Jacobucci et al., 2017). It is widely used in machine learning, image processing as well as pattern recognition (Yuping et al., 2018). Among them, gaussian mixture model is the earliest finite mixture model studied, which has the advantages of simple form and convenient calculation (Paetz and Steiner, 2017). However, in practice, most of the data are nonlinear and non-gaussian, so the gaussian mixture model can't completely, accurately and effectively describe these complex data (Al-Moisheer et al., 2017). Therefore, the research on FMM is also developed into more mathematical methods (Martella and Marco, 2017). Lassen et al. proposed a fast as well as semi-automatic sub surface nodule segmentation method, which provides satisfactory segmentation results with the minimum observation force in the shortest time, and can reduce the subjectivity of nodule segmentation under the clinical routine (Lassen et al., 2015). Chen et al. set the threshold to divide the image into two groups. One gray set corresponds to the target, and the other to the background. Then, the appropriate threshold is selected to maximize the variance between the two gray values, and get a good classification effect (Chen et al., 2014).

The accurate segmentation of pulmonary nodules can provide doctors with reliable auxiliary diagnosis basis. The accuracy of existing lung nodule segmentation algorithms needs to be well developed. In this study, 120 clean healthy rats were taken as the object, for the shortcomings of existing lung nodule segmentation algorithms, the research has been carried out, so as to improve the efficiency as well as accuracy of diagnosis. The innovation of this study is to optimize and improve the lung nodule segmentation method on the basis of the finite mixture model, further improve the accuracy of lung nodule segmentation, and provide necessary auxiliary diagnostic information for clinical diagnosis.

2. Materials and methods

2.1. Research object

There were 120 clean grade SD (Sprague Dawley) rats, half male and half female, 6–8 weeks old, weighing about 200 g. Rats were fed in separate cages, and there were 4 rats in each cage. National standard rodent feed was used. Rats could eat and drink freely. In terms of the body weight in the two groups, there was no significant difference. With natural light, the room temperature was at 20–26 °C, and the humidity was at 40–50%. After 2 weeks of adaptive feeding, rats were randomly divided into experimental group (120 rats) and control group (20 rats). Animal experiments were conducted in accordance with the *International Regulations for the Protection and Management of Animals* and approved by the respective ethics committee.

2.2. Establishment of lung cancer rat model

Rats in the experimental group were given 100 ppm diethylnitrosamine (Shanghai McLin Biochemical Technology Co., Ltd., China) daily to induce lung cancer and establish a lung cancer model. The rats in the control group were given regular drinking water for 16 weeks. Hispeed NX/i dual-spiral CT scanner (General Electric, USA) was used to perform CT imaging on rats, ranging from the upper thoracic cavity to the upper abdomen. The scanning parameters were as follows: 120 kV of tube voltage, 60 mA of tube current, 2 mm of layer thickness, and 2 mm of layer spacing.

2.3. Preprocessing of CT images

The CT image data of successfully modeled rats were preprocessed. In the process of image acquisition, due to optical system distortion, relative motion, atmospheric flow and rats' own physiological movement and other influencing factors, the image may be mixed with noise, causing noise pollution and blurring the image quality. Median filtering algorithm is a nonlinear signal processing technique based on sorting statistics theory. It was necessary to reduce the noise of CT images and then conduct image binarization by Otsu method. According to the gray-scale characteristics of the image, the image is divided into background as well as target. The larger the inter-class variance between the two, the greater the difference. When some targets or backgrounds are misclassified, the difference between background and target becomes smaller. Therefore, the segmentation with the largest inter-class variance means that the probability of wrong segmentation reaches the minimum. Background was filled to extract the left and right pulmonary parenchyma, and intraparenchymal nodules and vascular areas were filled to remove interfering information. The maximum connected domain method was used to determine whether there was adhesion in the left and right lung parenchyma. After identifying the area of adhesion, it was defined as the location of the valley floor of pixel distribution, and the left and right lung parenchyma were separated according to the pixel distribution map.

2.4. Image segmentation algorithm based on FMM

Gaussian Mixture Model (GMM) refers to the model that accurately quantizes things by Gaussian probability density function (also known as normal distribution curve). The probability density function is shown in Eq. (1).

$$F_{GS}(x_i|\Theta) = \sum_{j=1}^{k} w_j p(x_i|\Theta) \tag{1}$$

In the equation, x_i represents the i-th random variable (i = 1,2, ... n) in the image. $p(x_i|\Theta)$ is the probability density function corresponding to each component (i = 1, 2, ... k) and all of them obey Gaussian distribution. Θ represents the parameter set of GMM.

Gamma distribution refers to the probability density of earthquake occurrence time i that can be obtained when the earthquake sequence is orderly, the earthquake incidence is homogeneous, and the counting characteristics are independent increment and steady increment. The probability density function of Gamma mixed model is shown in equation (2).

$$F_{GA}(x_i|\Theta) = \sum_{j=1}^{k} w_j g(x_i|\Theta) \tag{2}$$

In the equation, x_i represents the i-th random variable (i = 1,2, ... n) in the image. $g(x_i|\Theta)$ is the probability density function corresponding to each component (i = 1,2, ... k), and they all obey Gamma distribution. Θ represents the parameter set of GMM.

In this experiment, gaussian mixture model and Gamma mixture model were used to fit the actual data, and adaptive particle swarm optimization (APSO) was used to optimize the number of mixed components as well as model parameters. The upper and lower bounds of the mixed component number of the finite mixing

model were set, and the parameter information and model component of the gaussian mixing model and Gamma mixing model were added to each particle, so that the particle had different vector lengths, and the effective mixed component number of the particle was obtained. The fitness value, difference, diversity, regression function and inertia weight of particles were calculated, all particles had the same vector length by the maximum selection method, and the maximum effective mixed component number was obtained, which was taken as the effective number of mixed component number of all particles.

2.5. Segmentation of pulmonary nodules on the basis of APSO algorithm-Gaussian mixture model (APSO-GMM)

CT image of pulmonary parenchyma is composed of pulmonary parenchyma, solid nodules, ground glass nodules and blood vessels. Gaussian mixed model was established based on gray scale characteristics of lung parenchyma, and gray scale probability density curve of CT image of lung parenchyma was obtained by adaptive particle swarm optimization. Gaussian mixed model was optimized, and fitness function was set. Through the negative logarithmic likelihood function and JS_{GS}, the optimal position of particles and global optimal position were updated, and the parameters were estimated repeatedly to obtain the convergence curve. The tissue within the lung parenchyma was accurately classified by the optimal distribution model to obtain potential areas of the pulmonary nodules. Support Vector Machine (SVM) is a kind of generalized linear classifier for binary classification of data according to supervised learning way. The potential areas of pulmonary nodules were screened by support vector machine to identify pulmonary nodules.

2.6. Segmentation of pulmonary nodules on the basis of APSO algorithm-Gamma mixed model (APSO-GaMM)

Gamma mixed model was established on the basis of gray scale characteristics of lung parenchyma, and gray scale probability density curve of CT image of lung parenchyma was obtained by adaptive particle swarm optimization. Gamma mixed model was optimized, and fitness function was set. The optimal position of particles and global optimal position were updated with the negative logarithmic likelihood function and JS_{GS}, and the parameters were estimated repeatedly to obtain the convergence curve. The tissue in lung parenchyma was classified by the optimal distribution model, and the potential areas of pulmonary nodules were screened by support vector machine to identify pulmonary nodules.

2.7. Segmentation of pulmonary nodules based on self-selected mixed distribution model of statistical information

K-means algorithm is a typical representative of the clustering method based on prototype objective function. It optimizes the distance between the data point and the prototype and obtains the adjustment rules of the iterative operation by the function of extremum. In this experiment, the k-means algorithm was used to initialize the self-selected mixed distribution model, and the dictionary-based Stochastic Expectation Maximization (DSEM) algorithm was improved by the stopping criteria and conditions. Firstly, the expression of logarithmic likelihood function was obtained by missing information, and the parameter estimation and conditional expectation of implicit variables were obtained by fitting mixed components of distribution function. The parameters and weights of the mixed model components were updated according to the posterior probability marker pixels. The optimal distribution function was obtained from the logarithmic likelihood function, the optimal model combination was used to accurately classify the tissues in the lung parenchyma, and the potential areas of pulmonary nodules were screened by support vector machine to identify pulmonary nodules.

2.8. Segmentation of pulmonary nodules based on self-selected mixed distribution model of neighborhood information

Gradient method is also known as steepest descent method. Firstly, initialization was performed to calculate the posterior probability of the pixel and the mixed component, accurately classify the pixel, and maximize the logarithmic likelihood of the distribution function by the gradient method to obtain the model parameter estimation. The parameter set of the model was adjusted to obtain the gray probability density curve, and then the potential area of pulmonary nodules was screened by support vector machine to identify pulmonary nodules.

2.9. Effect evaluation the of segmentation of pulmonary nodules

The Kolmogorov-Smirnov test (KS-test) is a test to compare a frequency distribution f(x) with a theoretical distribution g(x) or two observed value distributions. The Correlation Coefficient method is a test method for investigating the degree of linear correlation between variables. In this experiment, the parameter estimation of finite mixed model was evaluated by these two methods. If the finite-mixed model showed superiority in the two testing methods, it indicated that the parameter estimation effect was good. The Dice coefficient is a set similarity measure function. Relative ultimate measurement accuracy (RUMA) is a method to quantitatively analyze whether segmentation results meet the requirements. Dice coefficient and relative final measurement accuracy were used to randomly select 10 chest CT image data from chest CT image data of rats with lung cancer to evaluate the effects of the five methods, that is, the segmentation of pulmonary nodules on the basis of APSO-GMM, APSO-GaMM, the traditional self-selected mixed distribution model according to statistical information, the improved self-selected mixed distribution model according to statistical information, as well as the self-selected mixed distribution model according to neighborhood information. The higher the Dice coefficient of pulmonary nodules, the better the segmentation effect, while the lower the relative final measurement accuracy, the better the segmentation effect.

3. Results and discussion

3.1. Preprocessing results of CT images

As shown in Fig. 1, from the initial segmentation results of lung parenchyma obtained from CT original image (Fig. 1A) by image binarization and lung parenchyma extraction (Fig. 1B), it can be seen that compared with CT original image, left and right lung par-

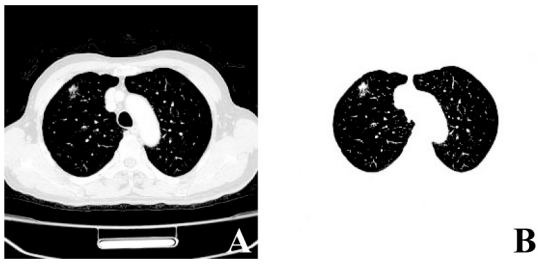

Fig. 1. Preprocessing results of CT images (A: original CT image; B: initial segmentation results of lung parenchyma).

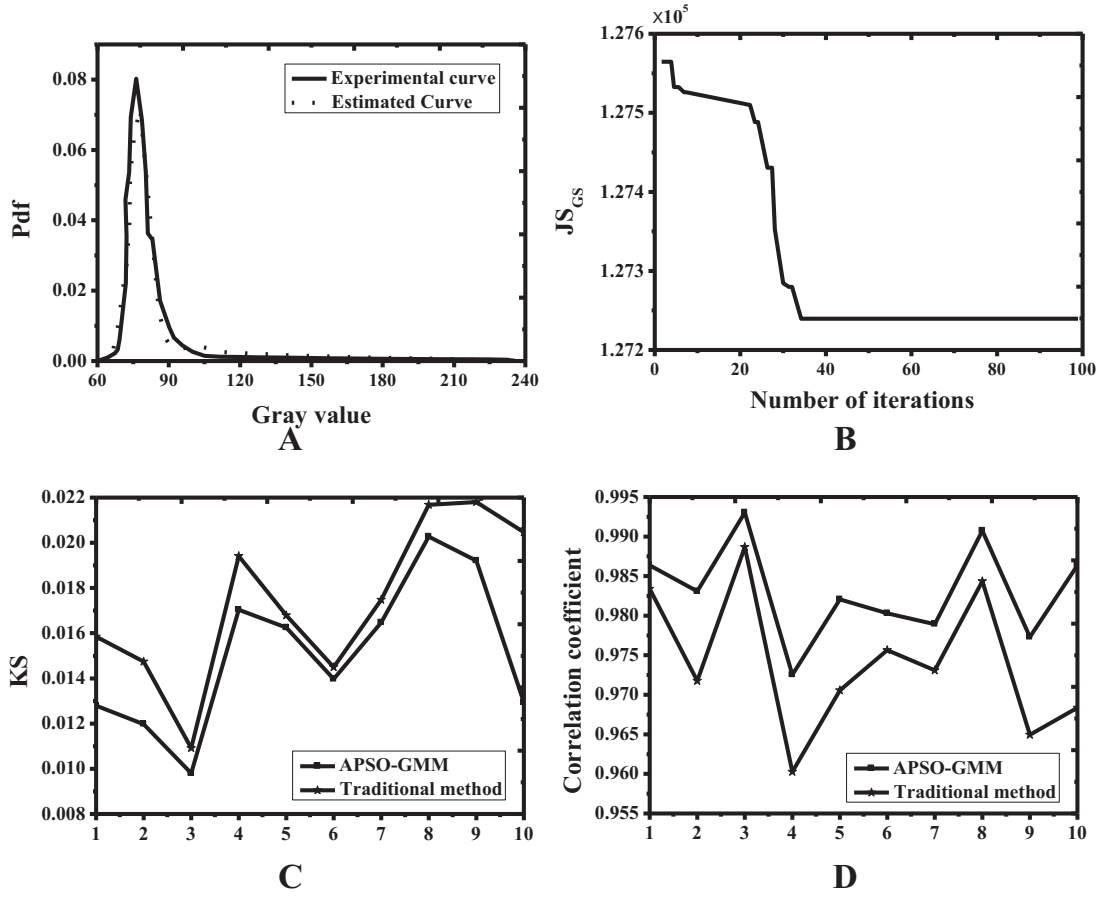

Fig. 2. Evaluation results of segmentation effect of pulmonary nodules based on APSO-GMM (A is the gray probability density curve of the CT image of the lung parenchyma; B is the convergence curve; C is the comparison of KS value with traditional methods; and D is the comparison of correlation coefficient with traditional methods).

Table 2
Comparison of segmentation results of pulmonary nodules based on APSO-GaMM and traditional methods.

Methods	Dice coefficient	RUMA value	Running time (s)
Traditional method	0.849736	0.168422	22.745
APSO-GMM	0.859943	0.150356	15.372

enchyma are separated, and the initial segmentation results of lung parenchyma are ideal.

3.2. Evaluation of segmentation effect of pulmonary nodules based on APSO-GMM

The results of segmentation effect of pulmonary nodules based on APSO-GMM are shown in Table 1 as well as Fig. 2. It can be concluded that the gray level probability density curve of CT images of lung parenchyma of segmentation of pulmonary nodule based on APSO-GMM was basically consistent with the estimated curve, and the KS value was lower than the traditional segmentation method on the whole, while the correlation coefficient was higher than the traditional method on the whole. The Dice coefficient of pulmonary nodule segmentation based on APSO-GMM was 0.854237, higher than that of the traditional method (0.848994), and its relative final measurement accuracy was 0.159763, lower than that of the traditional method (0.170247), indicating that the results of pulmonary nodule segmentation based on APSO-GMM were more accurate. Meanwhile, the pulmonary nodule segmentation based on APSO-GMM required a running time of 18.965 s, which was shorter than the traditional method (26.003 s). Therefore, the pulmonary nodule segmentation based on APSO-GMM was more advantageous.

Table 1
Comparison of segmentation results of pulmonary nodules based on APSO-GMM and traditional methods.

Methods	Dice coefficient	RUMA value	Running time (s)
Traditional method	0.848994	0.170247	26.003
APSO-GMM	0.854237	0.159763	18.965

3.3. Evaluation results of segmentation effects of pulmonary nodules based on APSO-GaMM

Evaluation results of segmentation effects of pulmonary nodules based on APSO-GaMM is shown in Table 2 as well as Fig. 3. It can be concluded that the gray level probability density curve of CT images of lung parenchyma of pulmonary nodule segmentation based on APSO-GaMM was basically consistent with the estimated curve, and the KS value was lower than the traditional segmentation method on the whole, while the correlation coefficient was higher than the traditional method on the whole. The Dice coefficient of pulmonary nodules segmentation based on APSO-GaMM was 0.859943, which was higher than that of the traditional method (0.849736), and its relative final measurement accuracy was 0.150356, which was lower than that of the traditional method (0.168422), indicating that the segmentation result of pulmonary nodules based on APSO-GaMM was more accurate.

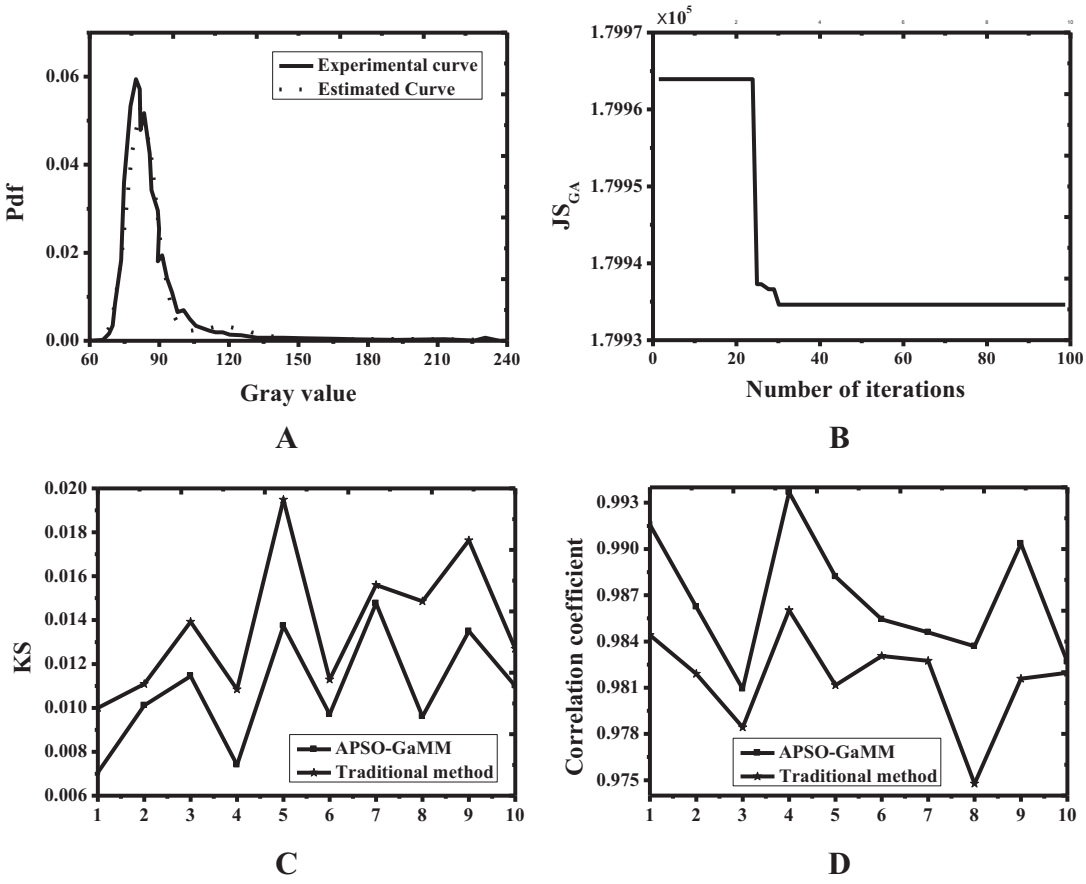

Fig. 3. Evaluation results of segmentation effect of pulmonary nodules based on APSO-GaMM (A is the gray probability density curve of the CT image of the lung parenchyma; B is the convergence curve; C is the comparison of KS value with traditional methods; and D is the comparison of correlation coefficient with traditional methods).

Table 3
Segmentation results of pulmonary nodule with self-selected mixed distribution model.

Method	Dice coefficient	RUMA value	Running time (s)
Traditional self-selected mixed distribution model	0.905032	0.138453	13.434
Improved self-selected mixed distribution model	0.911156	0.135641	10.064
Self-selective mixed distribution model based on neighborhood information	0.920034	0.106543	11.678

Meanwhile, the running time required by pulmonary nodule segmentation based on APSO-GaMM was 15.372 s, which was shorter than the traditional method (22.745 s). Therefore, pulmonary nodule segmentation based on APSO-GaMM was more advantageous.

3.4. Evaluation results of segmentation effects of pulmonary nodules based on self-selected mixed distribution model

The evaluation results of the segmentation effect of pulmonary nodules based on the self-selected mixed distribution model are shown in Table 3 as well as Fig. 4. It can be concluded that the gray level probability density curve of CT image of pulmonary parenchyma of pulmonary nodules segmentation based on the improved self-selected mixed distribution model according to statistical information was basically consistent with the estimated curve, the overall KS value was not much different from the traditional segmentation method, and the correlation coefficient was higher than the traditional method on the whole. Compared with the traditional method, the Dice coefficient of the improved self-selected mixed distribution model based on statistical information had little difference with the relative final measurement accuracy, indicating that the segmentation accuracy of the two methods had little difference. However, the improved method segmentation had shorter running time, higher segmentation efficiency, and better superiority. Compared with the results of pulmonary nodule segmentation in the self-selected mixed distribution model based on statistical information, the Dice coefficient of pulmonary nodule segmentation in the self-selected mixed distribution model based on neighborhood information was higher and the final measurement accuracy was smaller, which indicated that the self-selected mixed distribution model based on neighborhood information was more accurate, but it required longer running time and had lower efficiency.

3.5. Effects evaluation of five segmentation methods for pulmonary nodules

The results of five lung nodule segmentation methods, which are APSO-GMM, APSO-GaMM, traditional DSEM, improved DSEM, neighborhood information, were compared. The comparison results were shown in Fig. 5. The results showed that compared with the APSO-GMM and APSO-GaMM methods, the Dice value of the self-selected mixed distribution model was larger, and the relative final measurement accuracy was smaller, indicating that the segmentation accuracy of lung nodule of the self-selected mixed distribution model was higher. Among the five methods, the Dice value of the self-selected mixed distribution model based

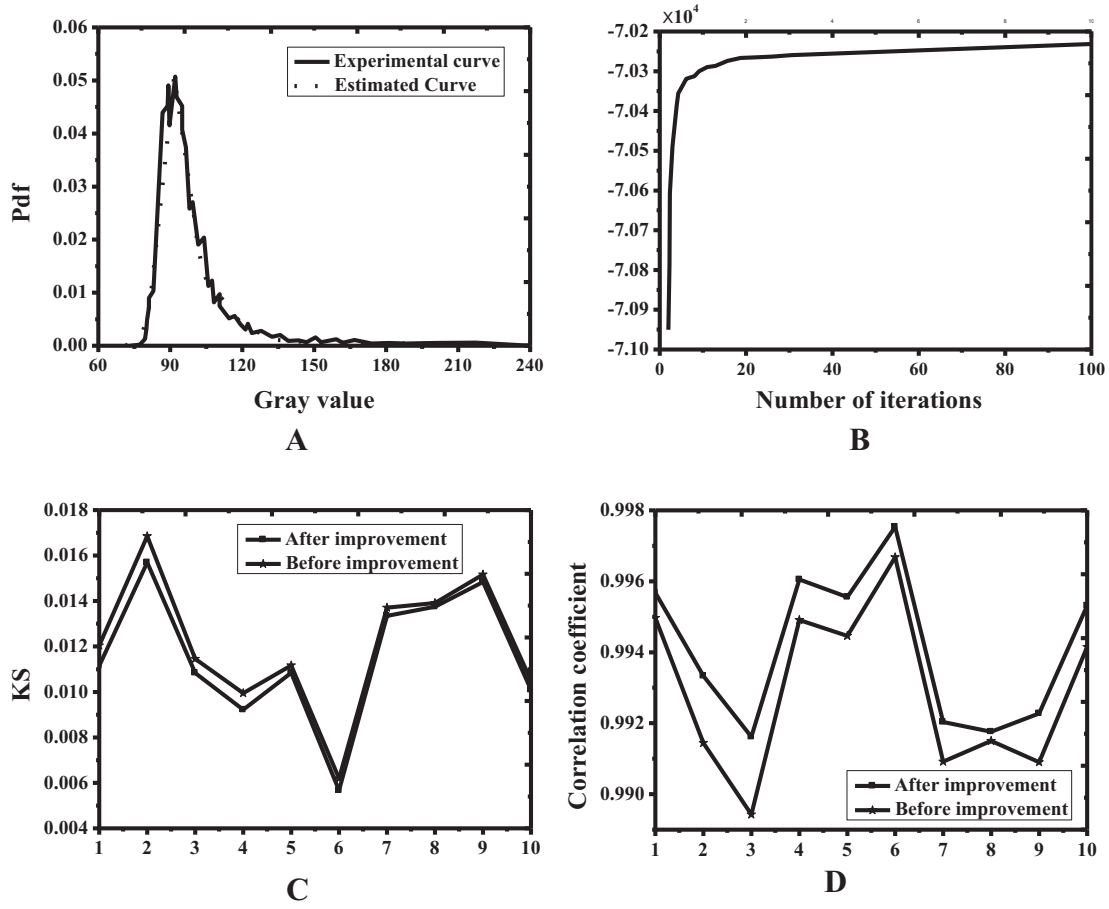

Fig. 4. Evaluation results of segmentation effects of pulmonary nodules based on self-selected mixed distribution model according to statistical information (A is the gray probability density curve of the CT image of the lung parenchyma; B is the convergence curve; C is the comparison results of KS value between improved method and traditional methods; and D is the comparison results of correlation coefficient between improved method and traditional methods).

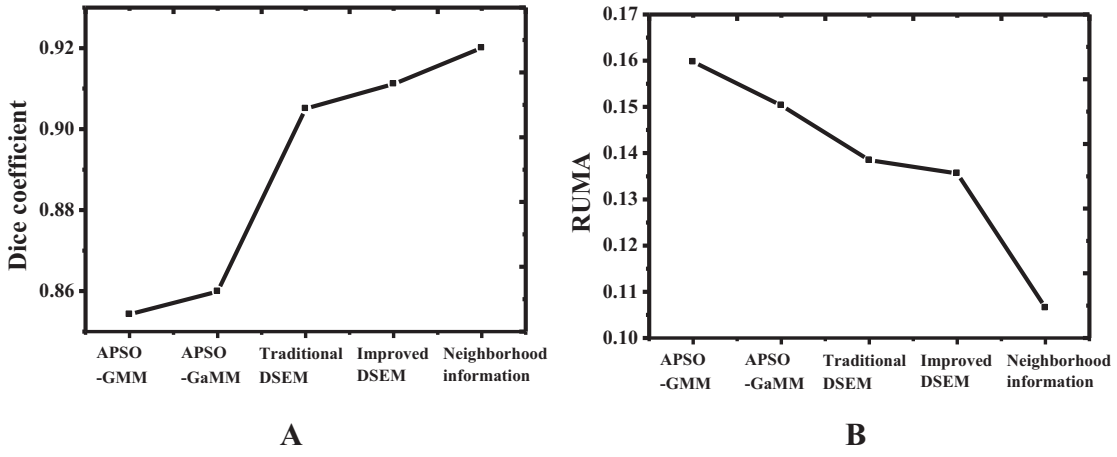

Fig. 5. Comparison of Dice coefficient values and relative final measurement accuracy for five segmentation methods (A is the comparison of the Dice value; and B is the comparison of the relative final measurement accuracy).

on neighborhood information was the largest and the relative measurement accuracy was the smallest, indicating that the segmentation effect of the self-selected mixed distribution model based on neighborhood information was the best.

4. Conclusion

In this study, the application of CT images when diagnosing lung cancer based on the finite mixture model is studied. By selecting 120 clean healthy rats as the research object, the lung cancer model is established and the lung CT image is examined. After preprocessing the chest CT image data successfully, image segmentation is carried out by different methods, and the segmentation effect is evaluated. Among them, the segmentation effect of self-selected mixed distribution model based on neighborhood information is the best, which provides reference for clinical lung cancer diagnosis. However, there are also some deficiencies in the study like the small samples size, which results in a certain degree

of deviation in the results. Therefore, it is necessary to increase the data capacity in the future to make the obtained results more reliable for reference.

Declaration of Competing Interest

The authors declare that they have no known competing financial interests or personal relationships that could have appeared to influence the work reported in this paper.

References

Yang, H.X., Woo, K.M., Sima, C.S., et al., 2017. Long-term survival based on the surgical approach to lobectomy for clinical stage I nonsmall cell lung cancer: comparison of robotic, video-assisted thoracic surgery, and thoracotomy lobectomy. Ann. Surg. 265 (2), 1.

Hui, R., Garon, E.B., Goldman, J.W., et al., 2017. Pembrolizumab as first-line therapy for patients with PD-L1-positive advanced non-small cell lung cancer: a phase 1 trial. Ann. Oncol. Off. J. Eur. Soc. Med. Oncol. 28 (4), 874–881.

Timmeren, J.E.V., Leijenaar, R.T.H., Elmpt, W.V., et al., 2017. Survival prediction of non-small cell lung cancer patients using radiomics analyses of cone-beam CT images. Radiother. Oncol. 123 (3), 363.

Lin, G.N., Peng, J.W., Liu, P.P., et al., 2017. Elevated neutrophil-to-lymphocyte ratio predicts poor outcome in patients with advanced non-small-cell lung cancer receiving first-line gefitinib or erlotinib treatment. Asia-pacific J. Clin. Oncol. 13 (5), 2696–2703.

Li, Q., Kim, J., Balagurunathan, Y., et al., 2017. CT imaging features associated with recurrence in non-small cell lung cancer patients after stereotactic body radiotherapy. Radiat. Oncol. 12 (1), 158.

Zhou, Y., Gao, S., Huang, Y., et al., 2017. A pilot study of18F-Alfatide PET/CT imaging for detecting lymph node metastases in patients with non-small cell lung cancer. Sci. Rep. 7 (1), 2877.

Vial, M.R., O'Connell, O.J., Grosu, H.B., et al., 2018. Diagnostic performance of endobronchial ultrasound-guided mediastinal lymph node sampling in early stage non-small cell lung cancer: a prospective study. Respirology (Carlton, Vic.) 23 (1), 76.

Ostrowski, M., Marjański, Tomasz, Rzyman, W., 2018. Low-dose computed tomography screening reduces lung cancer mortality. Adv. Med. Sci. 63 (2), 230–236.

Toyokawa, G., Kozuma, Y., Matsubara, T., et al., 2017. Radiological features of the surgically resected small-sized small-cell lung cancer on computed tomography. Anticancer Res. 37 (2), 877–882.

Jacobson, F.L., Jaklitsch, M.T., 2018. Computed tomography scanning for early detection of lung cancer. Annu. Rev. Med. 69 (1), 235–245.

Jacobucci, R., Grimm, K.J., Mcardle, J.J., 2017. A comparison of methods for uncovering sample heterogeneity: structural equation model trees and finite mixture models. Struct. Equ. Model. A Multidiscip. J. 24 (2), 270.

Yuping, L., Yuan, P., Wenda, H.E., et al., 2018. Variational Bayesian inference for finite inverted dirichlet mixture model and its application to object detection. Chinese J. Electron. 27 (3), 603–610.

Paetz, Friederike, Steiner, Winfried J., 2017. The benefits of incorporating utility dependencies in finite mixture probit models. Oper. Res.-Spektrum 39 (3), 1–27.

Al-Moisheer, A.S., Arfaoui, H., Maddouri, F., 2017. The asymptotic relative efficiency of a nonlinear discriminant function from a mixture of two inverse Weibull distributions. J. Comput. Theor. Nanosci. 14 (2), 1214–1221.

Martella, F., Marco, Alfò, 2017. A finite mixture approach to joint clustering of individuals and multivariate discrete outcomes. J. Stat. Comput. Simul. 87 (11), 1–21.

Lassen, B.C., Jacobs, C., Kuhnigk, J.M., et al., 2015. Robust semi-automatic segmentation of pulmonary subsolid nodules in chest computed tomography scans. Phys. Med. Biol. 60 (3), 1307–1323.

Chen, J.J., Zhao, D.C., Peng, C.L., et al., 2014. Comparative study on automatic lung parenchyma segmentation of CT data using improved OTSU and FCM methods. Space Med. Med. Eng. 27 (6), 448–452.